Published in final edited form as:
Phys Med Biol. 2010 January 21; 55(2): 339–363. doi:10.1088/0031-9155/55/2/002.

THE UF FAMILY OF REFERENCE HYBRID PHANTOMS FOR COMPUTATIONAL RADIATION DOSIMETRY

Choonsik Lee, PhD,
Division of Cancer Epidemiology and Genetics, National Cancer Institute, National Institute of Health, Bethesda, MD 20852

Daniel Lodwick, MS,
Department of Nuclear & Radiological Engineering, University of Florida, Gainesville, FL 32611

Jorge Hurtado, MS,
Department of Nuclear & Radiological Engineering, University of Florida, Gainesville, FL 32611

Deanna Pafundi, PhD,
Department of Nuclear & Radiological Engineering, University of Florida, Gainesville, FL 32611

Jonathan L. Williams, MD, and
Department of Radiology, University of Florida, Gainesville, FL 32611

Wesley E. Bolch, PhD
Departments of Nuclear & Radiological and Biomedical Engineering, University of Florida, Gainesville, FL 32611

Abstract

Computational human phantoms are computer models used to obtain dose distributions within the human body exposed to internal or external radiation sources. In addition, they are increasingly used to develop detector efficiencies for in-vivo whole-body counters. Two classes of the computational human phantoms have been widely utilized for dosimetry calculation: stylized and voxel phantoms, that describe human anatomy through mathematical surface equations and 3D voxel matrices, respectively. Stylized phantoms are flexible in that changes to organ position and shape are possible given avoidance of region overlap, while voxel phantoms are typically fixed to a given patient anatomy, yet can be proportionally scaled to match individuals of larger or smaller stature, but of equivalent organ anatomy. Voxel phantoms provide much better anatomical realism as compared to stylized phantoms which are intrinsically limited by mathematical surface equations. To address the drawbacks of these phantoms, hybrid phantoms based on non-uniform rational B-spline (NURBS) surfaces have been introduced wherein anthropomorphic flexibility and anatomic realism are both preserved. Researchers at the University of Florida have introduced a series of hybrid phantoms representing the ICRP Publication 89 reference newborn, 15-year, and adult male and female. In this study, six additional phantoms are added to the UF family of hybrid phantoms – those of the reference 1-year, 5-year, and 10-year child. Head and torso CT images of patients whose ages were close to the targeted ages were obtained under approved protocols. Major organs and tissues were segmented from these images using an image processing software, *3D-DOCTOR*™. NURBS and polygon mesh surfaces were then used to model individual organs and tissues after importing the segmented organ models to the 3D NURBS modeling software, *Rhinoceros*™. The phantoms were matched to four reference datasets: (1) standard anthropometric data, (2) reference organ masses from ICRP

For reprints and correspondence contact: Wesley E. Bolch, PhD, PE, CHP Director, Advanced Laboratory for Radiation Dosimetry Studies (ALRADS) Department of Nuclear and Radiological Engineering University of Florida, Gainesville, Florida 32611-8300 Phone: (352) 846-1361 Fax: (352) 392-3380 wbolch@ufl.edu.

Publication 89, (3) reference elemental compositions provided in ICRP 89 as well as ICRU Report 46, and (4) reference data on the alimentary tract organs given in ICRP Publications 89 and 100. Various adjustments and refinements to the organ systems of the previously described newborn, 15-year, and adult phantoms are also presented. The UF series of hybrid phantoms retain the non-uniform scalability of stylized phantoms while maintaining the anatomical realism of patient-specific voxel phantoms with respect to organ shape, depth and inter-organ distance. While the final versions of these phantoms are in a voxelized format for radiation transport simulation, their primary format is given as NURBS and polygon mesh surfaces, thus permitting one to sculpt non-reference phantoms using the reference phantoms as an anatomic template.

Keywords

NURBS; voxel; paediatric; hybrid phantom; radiation dosimetry

1. Introduction

Tissue absorbed dose in radiation dosimetry is generally assessed through Monte Carlo radiation transport simulation within a computational anatomic phantom. Similarly, these models may be used to simulate radioactively contaminated individuals to compute detector efficiencies for in-vivo counting systems. As medical imaging and computer technology have evolved, different types of computational phantoms have appeared. These phantom types include the first-generation stylized (or mathematical) phantoms (Cristy and Eckerman, 1987) and second-generation voxel (or tomographic) phantoms (Caon, 2004; Zaidi and Xu, 2007). More recently, third-generation hybrid (or a boundary-representation) phantoms have been introduced using non-uniform rational basis-spline (NURBS) and polygon mesh (PM) surfaces to describe anatomical structures (Lee *et al.*, 2007; Xu *et al.*, 2007; Segars *et al.*, 2008; Li *et al.*, 2008; Lee *et al.*, 2008).[1] Currently, hybrid phantoms provide the best features of stylized and voxel phantoms which include scalability to model individual patient body morphometry while maintaining a high degree of anatomic realism regarding organ shape, position, and depth within the body. Voxel phantoms provide scalability as well, as noted in studies by Veit and Zankl (1992) and by Caon et al. (2000), but these changes are generally limited to uniform variations in body size without changes in relative organ or body region anatomy.

Although children are more susceptible to the radiation-induced risks than are adults owing to their growing tissues and greater post-exposure life expectancy (BEIR, 2005), relatively few phantoms have been available to represent the paediatric population (Caon, 2004; Zaidi and Xu, 2007). This is partly because most radiation protection studies have focused on the adult worker population and partly because it is relatively difficult to obtain whole-body paediatric tomography images from which paediatric phantoms can be developed. Researchers at the University of Florida have been developing a series of paediatric voxel and hybrid phantoms. The University of Florida (UF) newborn voxel phantom was developed via image segmentation of a 6-day female newborn cadaver (Nipper *et al.*, 2002). Five head/torso voxel phantoms of different ages (9-month male, 4-year female, 8-year female, 11-year male, and 14-year male) were later constructed from head and torso computed tomography (CT) image data of live patients (Lee *et al.*, 2005). Arm and leg models segmented from an Korean adult male were attached to the head/torso phantoms to develop whole-body versions of these child phantoms (Lee *et al.*, 2006). Although these paediatric phantoms were anatomically more realistic as compared to previous stylized child phantoms (Cristy and Eckerman, 1987; Han *et al.*, 2006),

[1]The former define 3D surfaces via interpolation of a grid of weighted control points laid across the defined surface, with the latter defining these same surfaces via a series of adjacent triangular, quadrilateral, or other simple convex polygons.

they continued to display several drawbacks which could not be addressed by their voxel-based construction approach.

As part of a comprehensive effort to incorporate new hybrid technology into a series of computational phantoms where anatomical structures are described by NURBS or polygon mesh surfaces, the first whole-body hybrid phantoms were introduced in 2007 representing the reference newborn male and female of the International Commission on Radiological Protection (ICRP) (Lee *et al.*, 2007). In 2008, similar phantoms representing the ICRP reference 15-year-old male and female were also reported (Lee *et al.*, 2008). More recently, adult male and female hybrid phantoms were developed from patient CT data using the same technology (Hurtado *et al.*, in press). A total of four different reference data were incorporated into the series of hybrid phantoms: (1) the 50th percentile anthropometric data[2] collected from several different literature sources, (2) the reference organ masses from ICRP Publication 89 (ICRP, 2002), (3) the reference tissue densities and elemental compositions from both ICRP Publication 89 and Report 46 by the International Commission on Radiation Units and Measurements (ICRU) (ICRU, 1992), and (4) the reference alimentary tract data from ICRP Publications 89 and 100 (ICRP, 2006).

In this study, we present six new paediatric hybrid phantoms in the UF series – those representing ICRP 89 reference 1-year, 5-year, and 10-year male and female. Details regarding source images, developmental procedure, unique modeling issues, and resulting hybrid phantoms are reported. Revisions made to the four existing members of the UF hybrid phantom series are also discussed. While ICRP reference paediatric phantoms are of obvious interest to the radiological protection community, they can additionally be used as the anatomic template for non-uniform scaling to create an expanded library of patient-dependent phantoms as discussed by Johnson *et al* (in press) and Bolch *et al* (in press).

2. Materials and Methods

2.1. Development of 1, 5, and 10-year phantoms

2.1.1. Specification of CT image sets—The UF hybrid 1-year, 5-year, and 10-year phantoms were developed in part from the patient CT images used for the construction of the UF paediatric voxel phantom series (Lee *et al.*, 2006) and in part from newer CT datasets obtained from Shands Children's Hospital at the University of Florida (see Table 1). These phantoms were constructed using modeling procedures and organ identification lists given previously for the UF newborn and 15-year hybrid phantoms (Lee *et al.*, 2007; Lee *et al.*, 2008). The naming convention for the UF phantom series begins with the identifier UFH (University of Florida Hybrid), followed by the reference phantom age in years (00, 01, 05, 10, 15, and AD for adult), and then the phantom gender (M for male and F for female). The combined gender specification MF refers to the pair of male and female phantoms at the younger ages (newborn, 1-year, 5-year, and 10-year) where all internal organ anatomy is identical with the exception of the sex organs.

As shown in Table 1, original CT images used for the 4-year and 11-year UF voxel phantoms were reprocessed in this study for constructing hybrid phantoms representing the ICRP 89 reference 5-year and 10-year child. Patient CT image logbooks were reviewed under IRB-approved and HIPAA-compliant protocols to find the best candidates for reference phantom construction. Based on subject sex and age, a series of image sets were selected and then reviewed by the Chief of Paediatric Radiology at Shands Children's Hospital for abnormal patient anatomy (JW). All patients were scanned in a supine position with the arms raised to

[2]Value of the parameter (standing height, body mass, etc.) below which 50% of the population are found.

be out of the x-ray beam, and thus supplemental image sets were required to provide NURBS models for the skeleton of the extremities. Accordingly, separate arm bones (humerus, ulna, radius and hand bones) and leg bones (femur, patella, fibula, tibia and foot bones) were segmented from high-resolution CT images of an 18-year male cadaver and subsequently rescaled and attached to all phantoms of the series beyond the newborn. A total of 820 and 1099 images of the 18-year-old male cadaver CT datasets were semi-automatically segmented for construction of arm and leg models, respectively. Another supplementary image set was that of the cervical spine of a 15-year female patient. This image set, acquired at 0.75-mm slice thickness, yielded a far more discriminating view of the vertebral bodies and processes of the cervical spine than could be realized in existing 5-mm and 6-mm CT image sets used for the torso anatomy. Consequently, the resulting patient-specific cervical spine polygon mesh model was resized accordingly and inserted within the skeletal anatomy of all phantoms of the UF series older than the newborn.

2.1.2. Image segmentation for the 1-year, 5-year, and 10-year hybrid phantoms

—CT images were imported into the 3D image segmentation software, *3D-DOCTOR* to segment organs and tissues, which were later imported into the NURBS modeling tool, *Rhinoceros 4.0*™. Most organs and tissues were modeled with NURBS surfaces with the exclusion of the skeleton, brain, and extrathoracic airways which could be more effectively modeled by polygon mesh (PM) surfaces. The resulting phantoms are thus classified as hybrid-NURBS/PM phantoms.

The UF hybrid 1-year phantom was created using the head CT anatomy of a 2-year female (4.5-mm slice thickness) and the torso CT anatomy of a 1-year female (3-mm slice thickness). At one year of age, the cranial plates are not yet fused, and so fibrous connective tissue separating the cranial plates was modeled for this particular phantom using anatomical references as a guide (Schwartz, 2007; Steele and Bramblett, 1988). In addition, the 1-year female providing the torso images displayed a slight left-right scoliosis of the thoracic spine. Accordingly, the vertebral model was straightened in the NURBS/polygon mesh modeling stage taking advantage of the flexibility of these surface renderings. Adjacent organs such as the ribs, spinal cord, vertebral cartilage, esophagus, lungs, trachea, and kidneys were then repositioned around the new spinal location.

The UF hybrid 5-year phantom was created using the head and torso CT anatomy of a single 4-year female patient (5-mm slice thickness), while that of the UF hybrid 10-year phantom was assembled using the head CT anatomy of a 12-year male (6 mm slice thickness) and the torso CT anatomy of an 11-year male (6-mm slice thickness). While these slice thicknesses were sufficient to segment virtually all tissues and organs of the trunk, many of the finer features of the head anatomy, especially the craniofacial bones, could not be properly segmented. Consequently, *3D-Doctor*™ was used to provide interpolated 2-mm image data from the original 5-mm and 6-mm head CT image sets. The resulting cranial models provided for the UF hybrid 5-year and 10-year phantoms showed a higher level of facial bone detail than was inherent to the original UF voxel phantoms at similar ages.

The individuals whose head and torso images were used to create the 1-year, 5-year, and 10-year hybrid phantoms were a female, a female, and a male patient, respectively. Consequently, the corresponding 1-year male, 5-year male and 10-year female phantoms were created by replacing the segmented sex-specific organs with those of the opposite gender. The male-specific organs included the testes, penis, scrotum, prostate, and male urinary bladder, while the female organs included the ovaries, uterus, and female urinary bladder. Although the ICRP 89 reference masses of male and female urinary bladder are identical for the ages less than 15-year, their position and shape were modeled separately owing to the different position of adjacent sex organs within the male and female versions of these reference phantoms.

2.1.3. Scaling of hybrid phantoms to reference dimensions—Once provisional organ and tissue models were developed via NURBS and polygon mesh surfaces, the phantoms were matched to anthropometric data from several literature sources (see Table 2). A total of eight reference anthropometric parameters were employed: height (standing and sitting), length (total arm), biacromial breadth[3], and circumference (head, neck, waist, and buttock). Of these, ICRP Publication 89 provides only standing height for the 1-year, 5-year, and 10-year reference children. Sitting heights for 5-year and 10-year children, head circumferences for 1-year and 5-year children, buttock circumferences for 5-year and 10-year children, and biacromial breadths for 5-year and 10-year children were obtained from the National Health and Nutrition Examination Survey (NHANES) III (1988-1994) data series,[4] while other anthropometric data were provided by the database Anthrokids compiled by the U.S. Consumer Product Safety Commission.[5] Waist circumferences for 5-year and 10-year children were obtained from the NHANES IV (1999-2002) survey. As a result, only four parameters (standing and sitting height, arm length, and head circumference) were available for the 1-year phantoms. These same parameters were used for male and female phantoms at the same age. Once body dimensions were matched to standard anthropometric data, the organ and tissue masses were adjusted to match those provided by ICRP Publication 89 to within a tolerance of 1%. Reference densities were taken from ICRU Report 46 to calculate target organ volumes to which provisional organ and tissue models were matched. Detailed descriptions regarding organ/tissue standardization can be found in Lee et al. (2008).

Currently, reference lengths and masses for the alimentary tract organs (esophagus, small intestine, right, left, and rectosigmoid colon) are available from ICRP Publications 89 and 100, whereas reference wall thickness are not reported (see Table 3). As stated in the section 6.3.10 of ICRP Publication 89, the reference lengths are physiological lengths representing those measured in a living person. The values are usually less than corresponding anatomical lengths measured at autopsy or during surgical tissue removal. In this study, the lengths of the alimentary tract organs in the 1-year, 5-year, and 10-year phantoms were matched to their ICRP reference values to within a tolerance of 5% by adjusting the lengths of central trace of each segment, which in turn were obtained from the original patient CT images. Second, a NURBS pipe model with an appropriate radius was generated along these central tracks via a trial and error process until a realistic shape and curvature was obtained. The alimentary tract wall masses were then matched to the reference masses given in ICRP Publication 89 to within a tolerance of 1% with the exception of the small intestine (see section 2.1.1). The final intestinal and colon models were reviewed by our paediatric radiologist (JW).

The skin thicknesses (epidermis plus dermis) for the 1-year, 5-year, and 10-year reference phantoms were derived from three different reference parameters: (1) skin mass and (2) body surface area provided in the sections 2.3.1 and 10.4 of ICRP Publication 89, respectively, and (3) a reference skin density from ICRU Report 46. Derived thicknesses for the skin are shown in Table 4 for the UF hybrid phantom series. Reference skin volumes were first calculated from reference skin masses and tissue densities. Next, a derived skin thickness was taken as the ratio of the reference skin volume and associated surface area. This approach, however, yielded a sharp discontinuity in skin thicknesses between the 10-year and 15-year phantoms. In the original pulsed ultrasound study by Tan *et al* (1982) cited in ICRP Publication 89, however, these authors concluded that “skin thickness was found to increase linearly with age up to the age of 20 years.” Consequently, the UF study team thus made adjustments to these derived thicknesses at ages 5-year and 10-year to provide for a more continuous change in skin thickness with increasing phantom age as shown in the final row of Table 4.

[3]Distance between the lateral ends (acromion processes) of the left and right scapulae.
[4]http://www.cdc.gov/nchs/nhanes.htm
[5]http://www.itl.nist.gov/div894/ovrt/projects/anthrokids

2.2. Revisions to existing phantoms

2.2.1. Revisions to the alimentary tract model—Wall masses of the alimentary tract organs including the esophagus, small intestine, and colon were originally matched to reference values within a tolerance of 1% in the UF newborn, 15-year, and adult phantoms. In the development of corresponding alimentary tract models for the 1-year, 5-year, and 10-year reference phantoms, two problems were identified. First, the anterior portions of the small intestine and colon were found to extend beyond the medial reach of the rib cage. This problem was particularly noticeable when we attempted to rescale our reference adult phantom to match other members of the U.S. patient population at weight percentiles below the 50th percentile (Johnson *et al.*, in press). Second, anterior-posterior (AP) and posterior-anterior (PA) views of the small intestine revealed unrealistically large gaps in various segments of the organ. In the present study, both anomalies were corrected in existing phantoms (newborn, 15-year, adult male and female) as well as in the new phantoms of the present study. These corrections entailed compression of the small intestine and colon models in the AP direction, and enlargement of the radius of the small intestine NURBS pipe model, with a corresponding enlargement of lumen diameter. These changes were made possible by a relaxation of our tolerance for matching ICRP 89 wall masses from 1% to 5%. Further details are given below in section 3.

2.2.2. Other minor revisions—In our previous UF hybrid phantoms, no attempt was made to target the volumes of the left and right lung separately – only their combined volume and mass. Section 5.3.3 of ICRP Publication 89, however, states that the mass of the right lung is usually ~15% larger than that of the left lung. In this study, this ratio was applied to the targeted left/right lung volumes across all UF hybrid phantoms to within a tolerance of 5%.

The kidneys within the UF hybrid phantom series include three regions – a renal cortex, medulla, and pelvis – at relative volumes of 70%, 25%, and 5%, respectively, as per section 8.2.1 of ICRP Publication 89. In the UF newborn, 15-year, and adult phantoms, the summed masses of these three regions were targeted to ICRP 89 reference kidney mass at each corresponding reference age. However, upon further reflection, the pelvis should not be included in this mass estimate as it contain urine, and not kidney parenchyma, and would presumably not be included in an autopsy assessment of kidney mass. Consequently, the kidney models in the final UF phantom series are constructed so that only the renal cortex and renal medulla volumes comport with ICRP 89 reference kidney masses. The kidneys are thus treated similarly to that of the urinary bladder with both a wall and content mass.

In the previously published UF newborn, 15-year, and adult phantoms, reference masses for the salivary glands were matched according to the cumulative volumes of parotid, submaxillary, and sublingual glands in each phantom. Revisions made in this study include a refinement of the individual gland volumes so as to match reported mass ratios of 10:5:2 given in section 6.3.2 of ICRP Publication 89, each to within a tolerance of 1%.

A NURBS-based model of the teeth was designed and inserted into the appropriate position between cranium and mandible in all phantoms with the exclusion of the newborn and 1-year phantoms. Total masses were matched to reference masses given in the section 9.2.15 of ICRP 89. Tooth density in the newborn and 1-year phantoms is reflected in the average density of the homogenized skeleton. Correspondingly, the teeth are excluded from homogeneous bone in the older phantoms, and are given their own organ tag values and assigned material composition and density.

The original female breasts in the 15-year and adult female phantoms were modeled by two symmetric hemispheres. Upon further discussion and consideration, a more realistic asymmetric breast shape was applied to these older phantoms by reshaping the upper portion of each breast to include a higher placement on the chest wall.

3. Results and Discussion

3.1. Hybrid phantoms of the 1-year, 5-year, and 10-year reference children

The 1-year female, 5-year female and 10-year male phantoms were segmented from the patient CT data tabulated in the Table 1 using *3D-DOCTOR*™. The provisional phantoms were converted to NURBS and polygon mesh surfaces using *Rhinoceros*™. These phantoms were then made to conform to various reference dimension as shown in Table 3. Corresponding phantoms of the other gender were created by replacement of sex organs with those of the opposite sex. As an example, Figures 1A and 1B show the sex-specific organs in the 10-year male and female phantoms, respectively. The prostate, penis, testes, scrotum, and male urinary bladder wall and content were thus replaced by the ovaries, uterus, and female urinary bladder wall and content. As mentioned previously, the urinary bladder shape and position are slightly different in the two phantoms in order to accommodate the position and shape of surrounding sex organs.

The final NURBS/polygon mesh phantoms were voxelized using in-house MATLAB™ code, Voxelizer 6.0. The adjusted skin thicknesses tabulated in the final row of Table 4 were used to assign a targeted voxel size. Skin is generated by tagging the outer most voxel layer with skin tag number via an in-house IDL™ code, *Skin Generator*. Voxel array sizes of the resulting 1-year, 5-year, and 10-year voxel phantoms were thus 396 × 251 × 1156 (115 MB), 506 × 283 × 1585 (227 MB), and 514 × 269 × 1700 (235 MB), respectively.

Figures 2A to 3C show the transverse views of the 1-year, 5-year, and 10-year hybrid-voxel phantoms at the levels of lens (left), heart (middle), and the bottom of liver (right). Major organ indicators are included only for the 1-year phantom as these organ structures are similar at other ages. These images are not to scale with each other, but were adjusted proportionally by sitting height for better anatomical viewing. One can see from the left image in Figure 2A that the ethmoid bone is not completely ossified in the 1-year phantom while it is fully developed in two older phantoms. Figures 3 and 4 show the mid-coronal and mid-sagittal views, respectively, of the 1-year, 5-year, and 10-year male phantoms. As in Figure 2, these images are rescaled by sitting heights. The fibrous connective tissues separating the cranial plates are explicitly seen only in the 1-year phantom (see Figures 3A and 4A). Also evident in Figure 4 is fact that the head-to-torso size ratio decreases with increasing phantom age.

3.2. Revisions to the existing phantoms

The small intestine and colon were revised as described in the section 2.1.1. Figures 5A and 5B display an example of this change in the case of the adult male phantom before and after these revisions, respectively. Top images show the change in the anterior extension of the transverse colon in the lateral view which was made possible by compression of the small intestine model in the anterior-posterior direction. The tolerance to reference values when matching to the small intestine wall mass was changed from 1% to 5% which allowed more flexibility to the small intestine shape. The anterior extent of the transverse colon no longer extends beyond the frontal reach of the rib cage in the revised model. The central trace of small intestine was also adjusted to allow a greater filling of inter-segmental gaps of the abdominal cavity as shown in the bottom portions of Figure 5A and 5B. The same improvement was applied to all other hybrid phantoms of the UF series. The newly segmented parotid, submaxillary, and sublingual glands are shown in Figure 6A for the newborn head model. In Figure 6B, we show the revised models of the renal cortex, medulla, and pelvis within the newborn torso. For both organs, their individual sub-region masses were matched to ICRP Publication 89 reference values to within a tolerance of 1%.

3.3. UF series of hybrid phantoms

Important characteristics of the UF hybrid phantom series are presented in this section along with targeted reference values including (1) anthropometric data, (2) alimentary tract data, and (3) organ/tissue masses of the UF hybrid-NURBS/PM and hybrid-voxel phantom series.

3.3.1. Anthropometric data—Table 2 displays values of four body dimensions and four circumferences for the UF hybrid phantom series, along with their reference values and relative differences. All anthropometric parameters were matched to within a tolerance of 5%, yet many were matched to within only 1 to 2%. For the newborn phantom, the only parameters available included standing height (or length), sitting height (or crown-rump length), and head circumference. Reference values for biacromial breadth and circumferences of the neck, waist, and buttock were not available for the 1-year-old child. All eight reference anthropometric parameters were available for the older phantoms and used to standardize their body dimensions.

3.3.2. Alimentary tract data—Wall masses for the esophagus and colon (left, right, and rectosigmoid) were matched to their reference values given in ICRP Publication 89 to within a tolerance of 1%, while wall masses of small intestine were matched to within a tolerance of 5%. Furthermore, wall lengths of the esophagus, small intestine, and three colon segments were matched to ICRP 89 reference values to within a tolerance of 5%. Final values and their relative differences for alimentary tract lengths are given in Table 3 for the UF phantom series.

3.3.3. Organ masses of the NURBS/polygon mesh and voxel phantoms—Tissue densities and organ masses within the UF hybrid-NURBS/PM phantoms are tabulated in Table 5 along with their relative differences to ICRP 89 reference masses. For the newborn, 1-year, 5-year, and 10-year phantoms, organ masses are identical in both sexes, with the obvious exception of a few sex-specific tissues. In contrast, ICRP Publication 89 defines an gender-specific set of organ masses for the 15-year-old and adult, and so separate data columns are provided in Table 5 for male and female versions of these phantoms.

The assigned density of the alimentary tract content was determined as the ratio of the reference content mass and final lumen volume seen in corresponding UF hybrid phantom. These derived content densities were thus used to force the alimentary tract content masses to match their corresponding reference values, but only when that derived lumen density was less than or equal to 1.03 g cm^{-3}. When the derived content density was seen to be greater than 1.03 g cm^{-3} (which occurred when the phantom's lumen volume was smaller than desired), that density was set at its reference values of 1.03 g cm^{-3}, yielding an underestimate of reference content mass. This approach was applied to the contents of stomach, small intestine, and all three sections of the colon. Lumen contents for the gall bladder and urinary bladder were matched to their reference masses to within 1% except for the newborn and 1-year phantoms where their urinary bladders were already occupying all available space between the small intestine and pelvis. The heart content of the newborn phantom was not able to be matched to its reference masses owing to the small space allowed for heart volume. It was also difficult to find additional space for placement of the thymus in the 1-year phantom which resulted in a phantom thymus mass 46.4% less than its reference mass.

Tissue densities and organ masses of the corresponding series of UF hybrid-voxel phantoms are given in Table 6 where percent differences from reference values are generally less than 1% for most organs and tissues, except in a few unique cases as mentioned above. Residual Soft Tissue (RST) is taken to be all interior phantom volumes that are not explicitly occupied by previously identified and tagged organs and tissues. Its tissue composition is taken to be a volume-weighted average of bone-associated cartilage, separable fat, skeletal muscle,

separable connective tissues, fixed lymphatic tissues, major blood vessels, and a final category termed miscellaneous RST. The mass of this latter and final component of RST is adjusted upward or downward to force agreement to the reference individual's total body mass as given in ICRP Publication 89. As noted previously by Lee *et al* (2007), however, RST in the newborn phantom does not include bone-associated cartilage as this tissue is uniquely provided as a thin layer covering the entire newborn skeleton.

The final four rows of Table 6 give the masses and relative differences for both total body mass (TBM) and total body tissues (TBT) in each phantom of the UF hybrid series. Total body mass is the summed masses of all tissues, organs, and fluids within the reference individual. Total body tissues are defined as the total body mass less the content masses of alimentary tract organs, gall bladder, renal pelvis, and urinary bladder. Both cumulative tissue masses are matched to ICRP 89 reference values to within 2% for the UF newborn, 5-year, 10-year, 15-year male, and adult male hybrid phantoms. They are correspondingly matched to within 1% of reference values for the UF 1-year, 15-year female, and adult female phantoms.

3.3.4. Three-dimensional frontal views of UF hybrid phantoms—Frontal 3D views of the final series of the UF hybrid phantoms are presented in Figure 7. The heights of the phantoms were scaled to match reference heights for each age given in ICRP Publication 89. The skin was made semi-transparent to better show the internal anatomy of the UF hybrid phantom series.

4. Conclusions

A new class of computational human phantoms, called hybrid phantoms, has been developed at the University of Florida since 2006. Six new members of the UF phantom series – the reference male and female 1-year, 5-year, and 10-year child – as well as revised versions of previously published phantoms of the male and female newborn, 15-year adolescent, and adult, are presented in this study. To ensure that the UF hybrid phantom series are compliant with the definition of a reference phantom, four different datasets were consulted during phantom development: (1) reference anthropometric data obtained from literature sources including ICRP Publication 89, (2) reference organ masses given in ICRP Publication 89, (3) reference tissue elemental compositions provided in both ICRP Publication 89 and ICRU Report 46, and (4) reference alimentary tract data given in ICRP Publications 89 and 100. A tolerance of 1% was applied to the mass of organ models and 5% to the body dimensions, alimentary tract lengths, and small intestinal wall masses.

The UF hybrid phantom series is provided in two formats. The first is via NURBS and polygon mesh surface renderings, and is termed hybrid-NURBS/PM phantoms. The second are voxelized versions of these same reference phantoms and are termed hybrid-voxel phantoms. The latter are different from traditional voxel phantoms in that both the voxel size and total voxel number in a hybrid-voxel phantom is user-defined, and thus can be altered readily based upon the user application. For traditional voxel phantoms, the voxel size can also be reset (to represent individuals of different total sizes), but the number of voxels remains fixed along with the ability to define anatomical details. For hybrid phantoms, when average organ doses are required, a larger voxel size and thus smaller voxel array can be generated. If, however, dose distributions within internal organs are required, as in many radiotherapy applications, a finer voxel size and large voxel array can be generated from the original hybrid-NURBS/PM phantoms. Finally, as was noted in our previous publication on the UF newborn hybrid phantom (Lee *et al.*, 2007), the resulting hybrid-voxel phantom displays improved continuity of organ boundaries (as compared to traditional voxel phantoms) as viewed in not only the transverse plane (which is typically the plane used to construction of a voxel phantom from CT or MR images), but in the coronal and sagittal planes as well. The other advance of hybrid phantoms

over traditional voxel phantoms is the ability to rapidly and non-uniformly change the phantom's body size, shape, and extremity positions, thus permitting one to expand the definition of a "reference" phantom beyond that of a individual at 50th height/weight percentile, but to include other individuals of a worker or medical patient population that exhibit non-50th percentiles of either body mass or stature (Johnson *et al.*, in press). At the time of radiation transport simulation, however, a voxelized phantom is presently required, whether from a segmented medical image (traditional voxel phantom) or from a voxel filling of NURBS or PM surfaces (hybrid-voxel phantom). Advances in radiation transport codes, however, will one day permit the direct use of hybrid-NURBS/PM phantoms and other unstructured mesh geometries, thus maximizing the use of their unique features and attributes in both internal and external dose assessment.[6] Updates to the UF hybrid phantom series currently ongoing include (1) the sub-segmentation of skeleton into regions of cortical bone, trabecular spongiosa, and medullary marrow (Pafundi *et al.*, 2009), and (2) inclusion of a model of the lymphatic nodes (Lee *et al.*, in press). Other future updates will include the addition major blood vessels, airways of the respiratory tract, and differentiation of the glandular and adipose tissues of the breasts in the 15-year and adult female phantoms. Voxelized versions of these phantoms can be made available upon request through a non-disclosure agreement with the Corresponding Author.

Acknowledgments

This research was supported in part by Grants RO1 CA116743 and CO6 CA059267 from the National Cancer Institute, Grant R01 EB00267 from the National Institute of Biomedical Imaging and Bioengineering, Contract HHS-N2612-0090-0098P from the Radiation Epidemiology Branch of NCI, and Contract TKC 30-06-16601 from TKC Integrated Services, Inc.

This work was supported by NCI, NIBIB, and TKCIS

References

BEIR. Health risks from exposure to low levels of ionizing radiation: BEIR VII - Phase 2. National Research Council; Washington, DC: 2005.

Bolch W, Lee C, Wayson M, Johnson P. Hybrid computational phantoms for medical dose reconstruction. Radiat Environ Biophys. in press.

Caon M. Voxel-based computational models of real human anatomy: a review. Radiat Environ Biophys 2004;42:229–235. [PubMed: 14730450]

Caon M, Bibbo G, Pattison J. Monte Carlo calculated effective dose to teenage girls from computed tomography examinations. Radiat Prot Dosim 2000;90:445–448.

Cristy, M.; Eckerman, KF. Specific absorbed fractions of energy at various ages from internal photon sources. Oak Ridge National Laboratory; Oak Ridge, TN: 1987. ORNL TM-8381

Han E, Bolch W, Eckerman K. Revisions to the ORNL series of adult and pediatric computational phantoms for use with the MIRD schema. Health Phys 2006;90:337–356. [PubMed: 16538139]

Hurtado JL, Lee C, Lodwick D, Geode T, Williams JL, Bolch WE. Hybrid computational phantoms representing the reference adult male and adult female: Construction and applications to retrospective dosimetry. Health Phys. in press.

ICRP. ICRP Publication 89: Basic anatomical and physiological data for use in radiological protection - reference values. Ann ICRP 2002;32:1–277.

ICRP. ICRP Publication 100: Human alimentary tract model for radiological protection. Ann ICRP 2006;36:1–366. [PubMed: 17188182]

ICRU. ICRU Report 46: Photon, electron, proton and neutron interaction data for body tissues. International Commission on Radiation Units and Measurements; Bethesda, MD: 1992.

[6]Personal communication with Dr. Tim Goorley, X-3 MCC, Los Alamos National Laboratory, April 2009.

Johnson P, Whalen S, Wayson M, Juneja B, Lee C, Bolch W. Hybrid patient-dependent phantoms covering statistical distributions of body morphometry in the US adult and pediatric population. Proceedings of the IEEE. in press.

Lee C, Lee C, Williams JL, Bolch WE. Whole-body voxel phantoms of paediatric patients - UF Series B. Phys Med Biol 2006;51:4649–4661. [PubMed: 16953048]

Lee C, Lodwick D, Hasenauer D, Williams JL, Lee C, Bolch WE. Hybrid computational phantoms of the male and female newborn patient: NURBS-based whole-body models. Phys Med Biol 2007;52:3309–3333. [PubMed: 17664546]

Lee C, Lodwick D, Williams JL, Bolch WE. Hybrid computational phantoms of the 15-year male and female adolescent: applications to CT organ dosimetry for patients of variable morphometry. Med Phys 2008;35:2366–2382. [PubMed: 18649470]

Lee C, Pafundi DH, Kaufman K, Bolch WE. An algorithm for lymphatic node placement in hybrid computational phantoms - applications to radionuclide therapy dosimetry. Proceedings of the IEEE. in press.

Lee C, Williams J, Lee C, Bolch W. The UF series of tomographic computational phantoms of pediatric patients. Med Phys 2005;32:3537–3548. [PubMed: 16475752]

Li X, Samei E, Segars WP, Sturgeon GM, Colsher JG, Frush DP. Patient-specific dose estimation for pediatric chest CT. Med Phys 2008;35:5821–5828. [PubMed: 19175138]

Nipper JC, Williams JL, Bolch WE. Creation of two tomographic voxel models of paediatric patients in the first year of life. Phys Med Biol 2002;47:3143–3164. [PubMed: 12361215]

Pafundi D, Lee C, Watchman C, Bourke V, Aris J, Shagina N, Harrison J, Fell T, Bolch W. An image-based skeletal tissue model for the ICRP reference newborn. Phys Med Biol 2009;54:4497–4531. [PubMed: 19556686]

Schwartz, J. Skeletal keys: An introduction to human skeletal morphology, development, and analysis. Oxford University Press, Inc.; New York, NY: 2007.

Segars WP, Mahesh M, Beck TJ, Frey EC, Tsui BM. Realistic CT simulation using the 4D XCAT phantom. Med Phys 2008;35:3800–3808. [PubMed: 18777939]

Steele, DG.; Bramblett, CA. The anatomy and biology of the human skeleton. Texas A&M University Press, Inc.; College Station, TX: 1988.

Tan CY, Statham B, Marks R, Payne PA. Skin thickness measurement by pulsed ultrasound: its reproducibility, validation and variability. Br J Dermatol 1982;106:657–667. [PubMed: 7082570]

Veit R, Zankl M. Influence of patient size on organ doses in diagnostic radiology *Radiat*. Prot. Dosim 1992;43:241–243.

Xu XG, Taranenko V, Zhang J, Shi C. A boundary-representation method for designing whole-body radiation dosimetry models: pregnant females at the ends of three gestational periods--RPI-P3, -P6 and -P9. Phys Med Biol 2007;52:7023–7044. [PubMed: 18029991]

Zaidi H, Xu XG. Computational anthropomorphic models of the human anatomy: the path to realistic Monte Carlo modeling in radiological sciences. Annu Rev Biomed Eng 2007;9:471–500. [PubMed: 17298237]

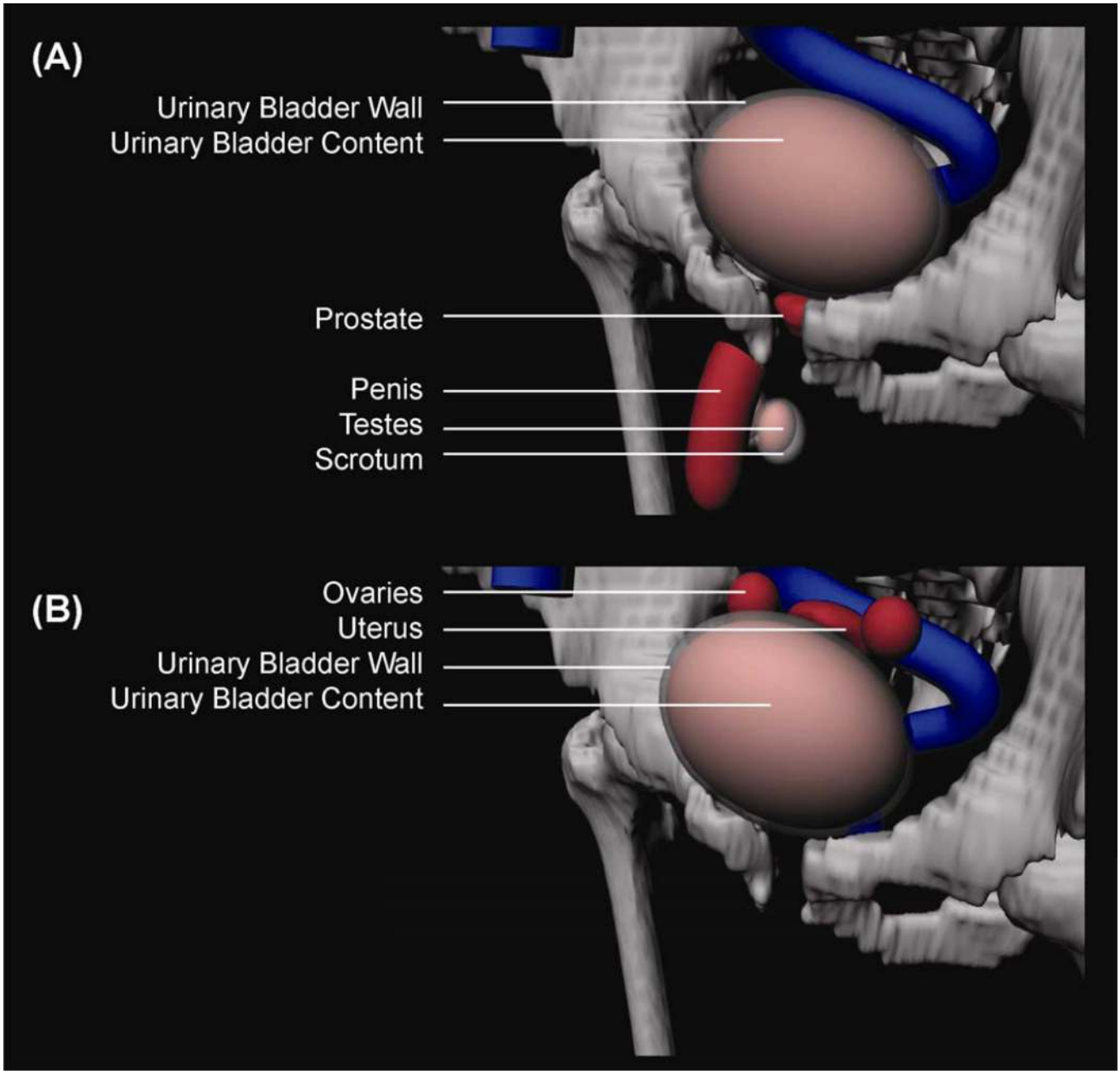

Figure 1.
Comparison of the placement of sex-specific organs within the pelvic region of the 10-year (A) male and (B) female UFH-NURBS/PM phantoms. The urinary bladder wall was made semi-transparent for viewing of the urinary bladder content.

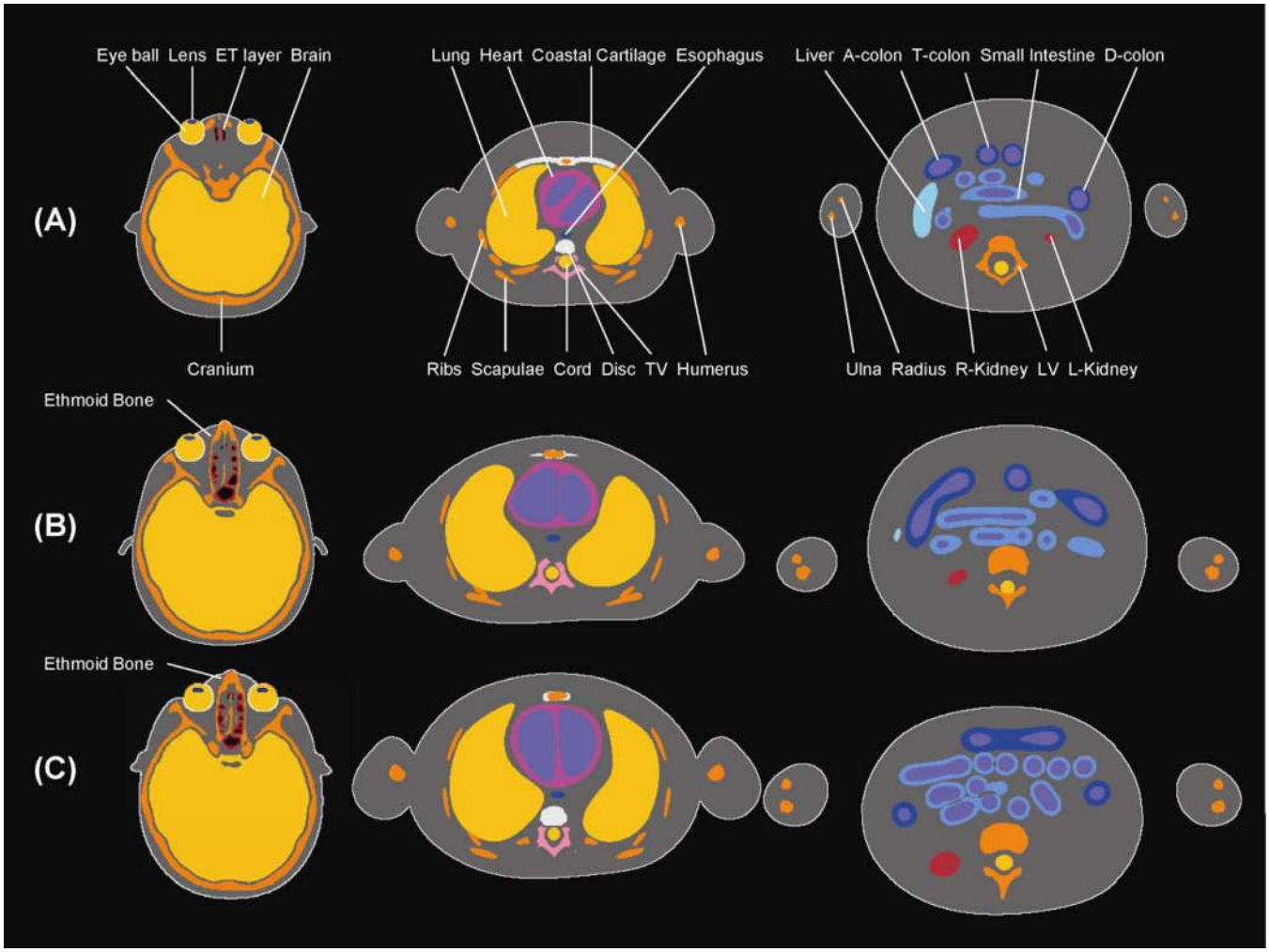

Figure 2.
Transverse views of the UFH-voxel (A) 1-year, (B) 5-year, and (C) 10-year male phantoms with major organs identified. For each phantom, the relative image scale was adjusted to give the appearance of equivalent sitting height.

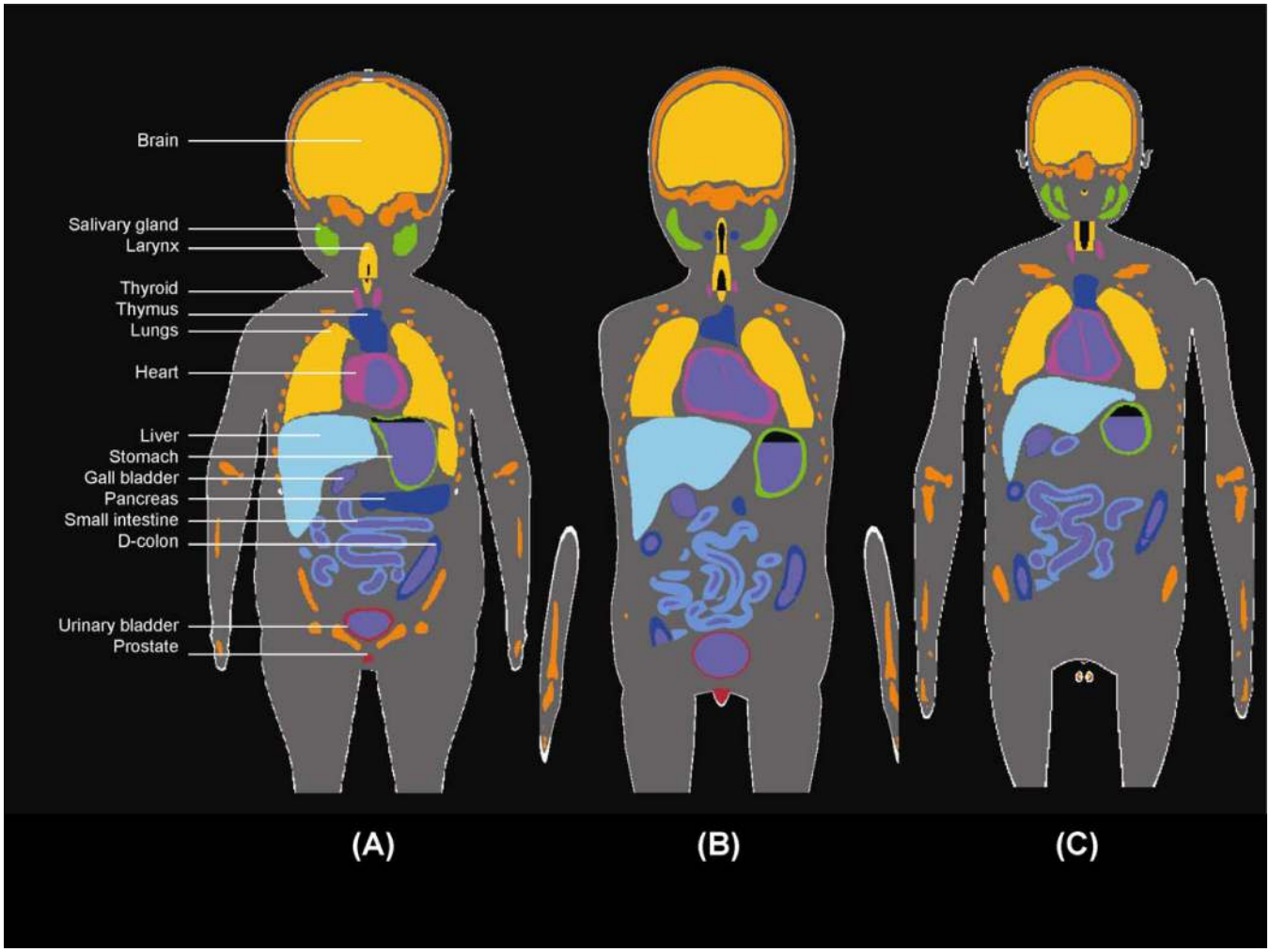

Figure 3.
Coronal views of the UFH-voxel (A) 1-year, (B) 5-year, and (C) 10-year male phantoms with major organs identified. For each phantom, the relative image scale was adjusted to give the appearance of equivalent sitting height.

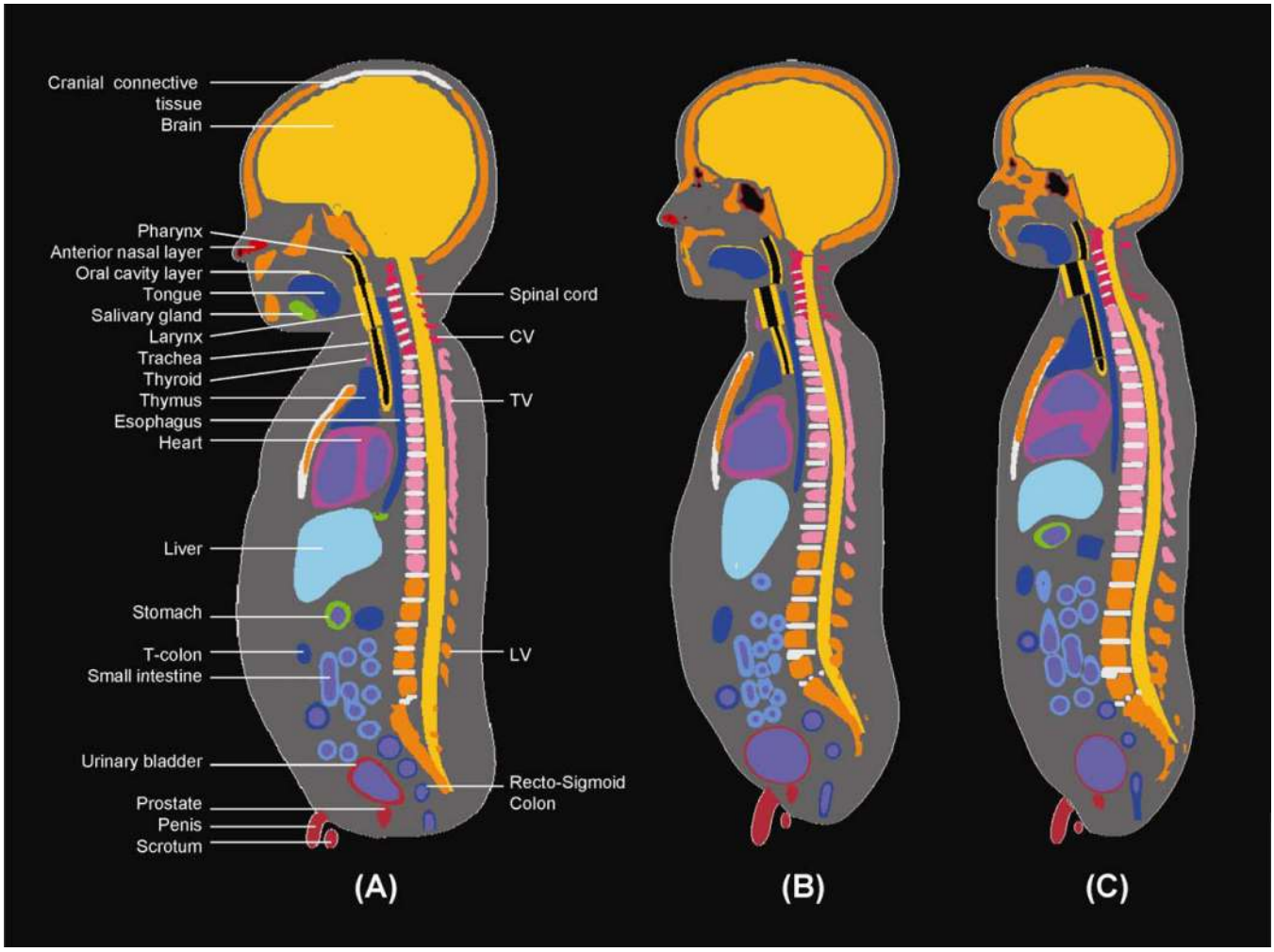

Figure 4.
Sagittal views of the UFH-voxel (A) 1-year, (B) 5-year, and (C) 10-year male phantoms with major organs identified. For each phantom, the relative image scale was adjusted to give the appearance of equivalent sitting height.

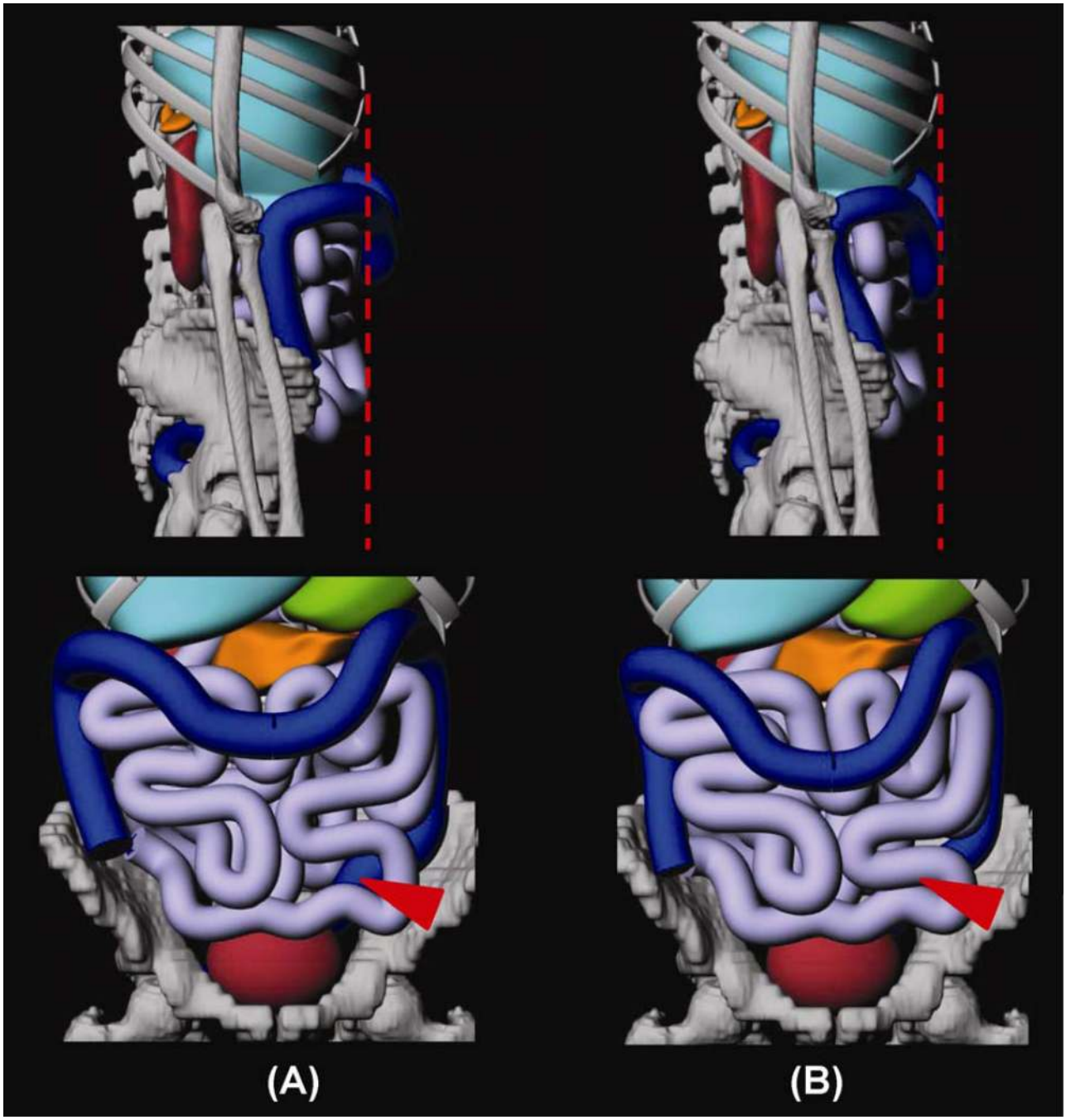

Figure 5.
3D views of the abdominal regions in the UFH adult male phantom (A) prior and (B) following model revisions to small and large intestine. The large intestine was moved medially (top panel) and the inter-intestinal gaps were filled by adjusting the central trace and small intestine diameters (bottom panel).

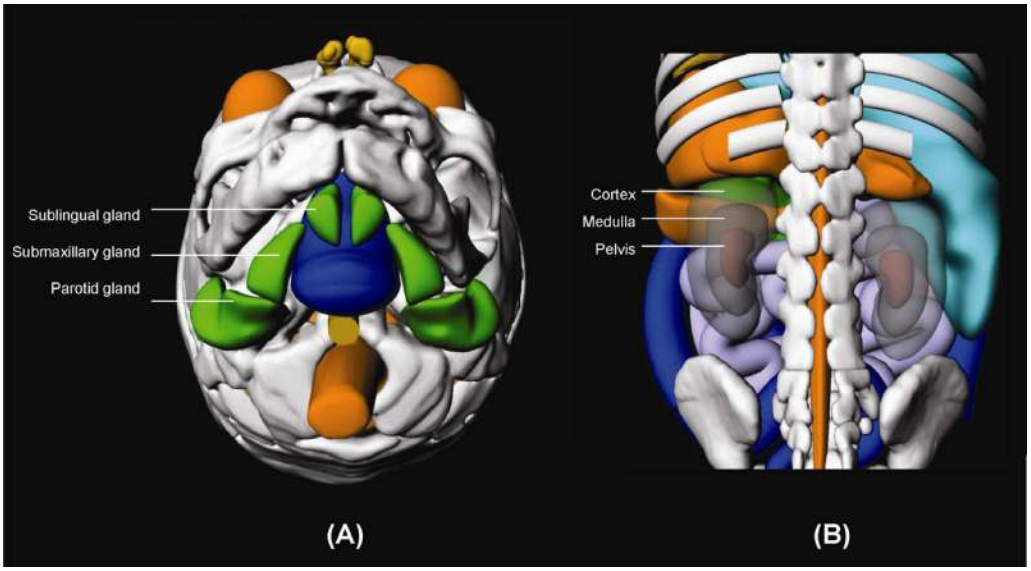

Figure 6.
Revised models of the (A) salivary glands and (B) kidneys in the newborn phantom.

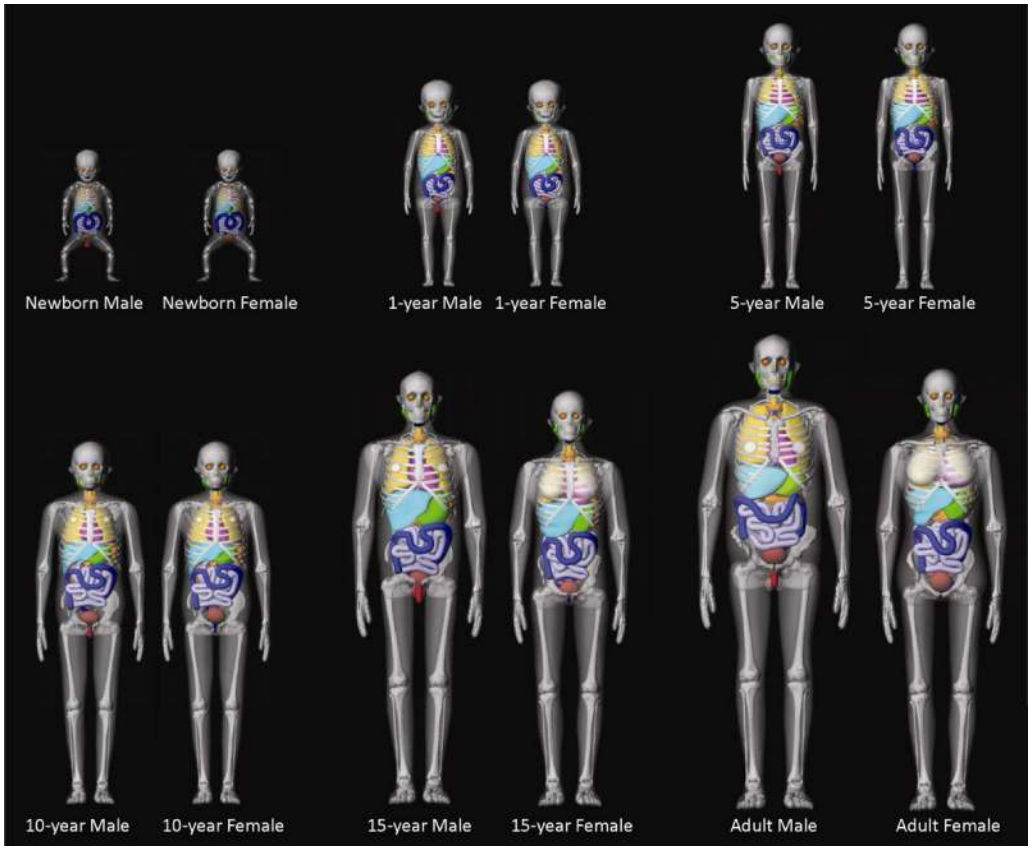

Figure 7.
3D frontal views of the entire series of UF hybrid paediatric and adult phantoms. The body contours were made semi-transparent for better viewing of internal anatomy.

Table 1

CT image sources employed in the development of the UF hybrid phantom series.

	Head	Torso	C-Vertebrae	Arms and Legs
UFH00MF	6-day F 0.586 × 0.586 × 1 mm^3			
UFH01MF	2-year F 0.379 × 0.379 × 4.5 mm^3	1-year F 0.406 × 0.406 × 3 mm^3		
UFH05MF	4-year F 0.451 × 0.451 × 5 mm^3			
UFH10MF	12-year M 0.469 × 0.469 × 6 mm^3	11-year M 0.469 × 0.469 × 6 mm^3		
UFH15M	18-year M[a] 1 mm	14-year M 0.625 × 0.625 × 6 mm^3	15-year F 0.21 × 0.21 × 0.75 mm^3	18-year M[c] 1 mm
UFH15F	15-year F 0.449 × 0.449 × 4.5 mm^3	14-year F 0.742 × 0.742 × 6 mm^3		
UFHADM	18-year M 1 mm	36-year M 1.97 × 1.97 × 3 mm^3		
UFHADF	15-year F[b] 0.449 × 0.449 × 4.5 mm^3	25-year F 0.66 × 0.66 × 5 mm^3		

[a] Head model of UFHADM was downscaled to UFH15M head model.

[b] Head model of UFH15F was upscaled to UFHADF head model.

[c] High resolution (1mm slice thickness) CT images of arms and legs were obtained from an 18-year male cadaver

Table 2

Comparison of reference and UF hybrid phantom values (cm) for various morphometric parameters regarding body size and shape.

Phantoms	*Standing Height*			*Sitting Height*			*Arm Length*			*Biacromial Breadth*		
	Ref.	UF	%Diff	Ref.	UF	%Diff	Ref.	UF	%Diff	Ref.	UF	%Diff
UFH00MF	51.0	51.0	0.0%	34.0	33.0	−2.9%						
UFH01MF	76.0	76.0	0.0%	48.8	47.3	−3.1%	32.6	32.0	−1.8%			
UFH05MF	109.0	109.0	0.0%	60.4	61.0	1.0%	47.1	47.0	−0.2%	25.0	24	−3.8%
UFH10MF	138.0	138.0	0.0%	73.4	75.2	2.5%	61.0	61.1	0.2%	31.2	30	−3.7%
UFH15M	167.0	167.0	0.0%	88.8	86.5	−2.6%	75.0	75.1	0.1%	38.8	37.2	−4.1%
UFH15F	161.0	161.0	0.0%	85.5	83.0	−2.9%	70.7	71.8	1.6%	36.3	35.4	−2.5%
UFHADM	176.0	176.0	0.0%	91.9	92.0	0.1%	80.1	80.9	1.0%	40.8	39.8	−2.5%
UFHADF	163.0	163.0	0.0%	86.1	85.5	−0.7%	73.5	72.9	−0.8%	36.4	35.8	−1.6%

Phantoms	*Head CC*			*Neck CC*			*Waist CC*			*Buttock CC*		
	Ref.	UF	%Diff	Ref.	UF	%Diff	Ref.	UF	%Diff	Ref.	UF	%Diff
UFH00MF	33.1	32.5	−1.8%									
UFH01MF	47.3	46.5	−1.7%									
UFH05MF	51.1	52.0	1.8%	24.9	24.3	−2.4%	55.0	57.0	3.7%	57.9	58.6	1.3%
UFH10MF	52.8	53.3	0.9%	27.9	27.1	−2.7%	66.7	70.0	4.9%	75.2	73	−2.9%
UFH15M	55.4	55.5	0.2%	32.8	32.2	−1.8%	80.1	83.0	3.6%	92.5	90.5	−2.2%
UFH15F	54.3	56.1	3.3%	30.8	31.0	0.6%	78.8	79.2	0.5%	93.4	93	−0.4%
UFHADM	57.2	57.4	0.3%	36.6	36.8	0.5%	92.5	92.1	−0.4%	96.0	96	0.0%
UFHADF	56.1	56.2	0.2%	31.4	31.9	1.6%	87.1	88.8	2.0%	97.6	95.6	−2.0%

Table 3

Comparison of alimentary tract lengths (cm) between ICRP Publication 100 reference values and those modeled in the UF hybrid phantom series.

Phantoms	*Esophagus*			*Small intestine*			*Right Colon*			*Left Colon*			*Sigmoid Colon*		
	Ref.	**UF**	**%Diff**	**Ref.**	**UF**	**%Diff**	**Ref.**	**UF**	**%Diff**	**Ref.**	**UF**	**%Diff**	**Ref.**	**UF**	**%Diff**
UFNBMF	10	10.2	2.4%	80	76.8	−4.1%	14	14.3	2.3%	16	16.4	2.5%	15	14.4	−4.0%
UF01MF	13	13.6	4.4%	120	115.8	−3.5%	18	17.1	−4.9%	21	20.1	−4.4%	21	20.0	−4.8%
UF05MF	18	17.8	−0.8%	170	163.3	−3.9%	23	22.9	−0.5%	26	24.9	−4.2%	26	27.0	3.8%
UF10MF	23	22.5	−2.0%	220	211.3	−4.0%	28	28.9	3.3%	31	30.6	−1.3%	31	29.6	−4.6%
UF15M	27	27.3	1.3%	270	257.8	−4.5%	30	30.7	2.2%	35	33.8	−3.3%	35	34.2	−2.3%
UF15F	26	26.8	2.9%	260	250.0	−3.8%	30	30.4	1.4%	35	35.5	1.3%	35	34.9	−0.3%
UFADM	28	28.4	1.5%	280	270.3	−3.5%	34	34.2	0.5%	28	28.2	0.7%	38	36.9	−3.0%
UFADF	26	26.2	0.7%	260	247.6	−4.8%	30	31.1	3.6%	35	34.9	−0.2%	35	33.7	−3.7%

Phys Med Biol. Author manuscript; available in PMC 2010 January 21.

Table 4

Reference anatomical parameters from ICRP Publication 89 used to derive reference skin thicknesses. An adjusted skin thickness to address the discontinuity between derived reference values for the 10-year and 15-year phantoms is also shown.

Anatomical Parameters	*Reference*	*UFH00*		*UFH01*		*UFH05*		*UFH10*		*UFH15*		*UFHAD*	
		M	**F**	**M**	**F**	**M**	**F**	**M**	**F**	**M**	**F**	**M**	**F**
Skin mass (g)	*Section 2.3.1 of ICRP89*	175	175	350	350	570	570	820	820	2000	1700	3300	2300
Surface area (m^2)	*Section 10.4 of ICRP89*	0.24	0.24	0.48	0.48	0.78	0.78	1.12	1.12	1.62	1.55	1.90	1.66
Density (g/cm^3)	*Section 10.6 of ICRP89*	1.10	1.10	1.10	1.10	1.10	1.10	1.10	1.10	1.10	1.10	1.10	1.10
Skin Volume (cm^3)		159.09	159.09	318.18	318.18	518.18	518.18	745.45	745.45	1818.18	1545.45	3000.00	2090.91
	Derived Skin Thickness (cm)	0.0663	0.0663	0.0663	0.0663	0.0664	0.0664	0.0666	0.0666	0.1122	0.0997	0.1579	0.1260
	Adjusted Skin Thickness (cm)	0.0663	0.0663	0.0663	0.0663	0.0697	0.0697	0.0824	0.0824	0.1122	0.0997	0.1579	0.1260

Table 5

89 reference values for tissues in the UF hybrid-NURBS phantom series.

UFH05MF			*UFH10MF*			*UFH15M*			*UFH15F*			*UFHADM*			*UFHADF*		
%Diff	**Density**	**Mass**	**%Diff**	**Density**	**Mass**	**%Diff**	**Density**	**Mass**	**%Diff**	**Density**	**Mass**	**%Diff**	**Density**	**Mass**	**%Diff**	**Density**	**Mass**	**%Diff**
0.0%	1.03	0.50	0.0%	1.03	0.52	0.0%	1.03	0.35	0.0%	1.02	0.51	0.0%	1.03	2.25	0.0%	1.02	0.62	0.0%
0.0%	1.03	8.79	0.0%	1.03	9.19	0.0%	1.03	14.05	0.0%	1.02	9.11	0.0%	1.03	20.61	0.0%	1.02	9.78	0.0%
0.0%	1.03	1.17	0.0%	1.03	1.02	0.0%	1.03	5.14	0.0%	1.02	7.89	0.0%	1.03	2.04	0.0%	1.02	1.79	0.0%
0.0%	1.07	7.00	0.0%	1.07	12.00	0.0%	1.07	22.03	0.1%	1.07	14.99	−0.1%	1.07	28.12	0.4%	1.07	19.00	0.0%
0.0%	1.03	1.93	0.0%	1.03	2.02	0.0%	1.03	5.79	0.0%	1.02	0.00	0.0%	1.03	2.27	0.0%	1.02	1.55	0.0%
0.0%	1.07	2.50	0.0%	1.07	4.52	0.4%	1.07	7.49	−0.1%	1.07	6.00	0.1%	1.07	10.06	0.6%	1.07	7.99	−0.1%
0.0%	1.07	0.00	0.0%	1.07	3.62	0.0%	1.07	7.99	0.0%	1.07	7.94	0.0%	1.07	16.55	0.0%	1.07	10.43	0.0%
0.0%	0.39	300.00	0.0%	0.33	500.00	0.0%	0.32	900.00	0.0%	0.31	750.00	0.0%	0.33	1200.00	0.0%	0.34	950.00	0.0%
0.0%	1.05	19.01	0.0%	1.05	32.00	0.0%	1.05	55.94	−0.1%	1.05	53.02	0.0%	1.05	73.16	0.2%	1.05	60.00	0.0%
0.0%	1.03	34.00	0.0%	1.03	44.00	0.0%	1.03	68.02	0.0%	1.02	65.03	0.0%	1.03	85.08	0.1%	1.02	70.06	0.1%
0.0%	1.03	2.00	0.0%	1.03	3.00	0.0%	1.03	3.01	0.3%	1.02	3.00	0.0%	1.03	3.02	0.5%	1.02	3.00	−0.1%
−0.2%	1.03	10.00	0.0%	1.03	18.00	0.0%	1.03	29.96	−0.1%	1.03	30.15	0.5%	1.03	39.95	−0.1%	1.03	35.00	0.0%
0.0%	1.03	50.00	0.0%	1.03	85.00	0.0%	1.03	119.71	−0.2%	1.03	120.07	0.1%	1.03	150.41	0.3%	1.03	140.00	0.0%
0.0%	1.03	83.23	0.3%	1.03	116.99	0.0%	1.03	200.47	0.2%	1.02	200.05	0.0%	1.03	250.13	0.1%	1.02	230.04	0.0%
2.9%	1.03	220.01	0.0%	1.03	370.06	0.0%	1.03	522.46	0.5%	1.03	520.09	0.0%	1.03	650.04	0.0%	1.03	599.99	0.0%
−59.2%	1.03	39.05	−66.6%	0.54	163.00	0.0%	0.41	280.00	0.0%	0.45	280.00	0.0%	0.44	350.00	0.0%	0.52	280.00	0.0%
0.0%	1.03	49.00	0.0%	1.03	84.99	0.0%	1.03	122.00	0.0%	1.03	122.00	0.0%	1.03	150.00	0.0%	1.03	145.00	0.0%
−61.4%	1.03	25.08	−49.8%	1.03	70.28	0.4%	1.03	72.51	−39.6%	1.02	43.93	−63.4%	1.03	100.66	−32.9%	1.02	51.68	−67.7%
0.0%	1.03	49.00	0.0%	1.03	85.00	0.0%	1.03	122.09	0.1%	1.03	122.00	0.0%	1.03	150.00	0.0%	1.03	145.00	0.0%
0.0%	0.76	25.00	0.0%	0.49	35.00	0.0%	0.34	60.00	0.0%	0.98	60.00	0.0%	1.03	55.24	−26.3%	1.08	80.00	0.0%
0.0%	1.03	21.99	−0.1%	1.03	40.02	0.0%	1.03	56.08	0.1%	1.03	55.98	0.0%	1.03	70.01	0.0%	1.03	70.02	0.0%
−27.3%	0.86	25.00	0.0%	1.03	32.01	−8.6%	0.49	60.00	0.0%	1.02	52.11	−13.1%	0.97	75.00	0.0%	1.02	56.12	−29.8%
0.0%	1.05	570.00	0.0%	1.05	830.00	0.0%	1.05	1300.27	0.0%	1.05	1301.26	0.1%	1.06	1802.64	0.1%	1.06	1399.05	−0.1%

UFH05MF			*UFH10MF*			*UFH15M*			*UFH15F*			*UFHADM*			*UFHADF*		
%Diff	**Density**	**Mass**	**%Diff**	**Density**	**Mass**	**%Diff**	**Density**	**Mass**	**%Diff**	**Density**	**Mass**	**%Diff**	**Density**	**Mass**	**%Diff**	**Density**	**Mass**	**%Diff**
−0.3%	1.03	2.60	0.0%	1.03	4.40	0.0%	1.03	7.69	−0.1%	1.02	7.34	0.6%	1.03	10.05	0.5%	1.02	7.99	−0.1%
0.1%	1.03	15.00	0.0%	1.03	26.00	0.0%	1.03	45.00	0.0%	1.02	42.02	0.0%	1.03	58.02	0.0%	1.02	48.02	0.0%
0.0%	1.03	35.00	0.0%	1.03	60.00	0.0%	1.03	110.00	0.0%	1.02	100.06	0.1%	1.03	140.10	0.1%	1.02	120.00	0.0%
0.4%	1.04	85.00	0.0%	1.04	140.00	0.0%	1.04	230.13	0.1%	1.04	219.93	0.0%	1.05	330.20	0.1%	1.05	250.01	0.0%
0.0%	1.06	135.00	0.0%	1.06	230.00	0.0%	1.06	429.88	0.0%	1.06	320.09	0.0%	1.06	509.44	−0.1%	1.06	370.00	0.0%
−0.2%	1.04	109.99	0.0%	1.04	180.00	0.0%	1.04	249.94	0.0%	1.04	239.78	−0.1%	1.05	309.81	−0.1%	1.05	274.82	−0.1%
−0.5%	1.01	5.62	0.0%	1.01	9.20	0.0%	1.01	12.80	0.1%	1.01	12.26	0.0%	1.01	15.69	0.0%	1.01	13.91	−0.1%
0.1%	1.04	16.00	0.0%	1.04	25.00	0.0%	1.04	39.99	0.0%	1.04	35.01	0.0%	1.04	50.12	0.2%	1.04	40.15	0.4%
−68.4%	1.01	62.00	0.0%	1.01	99.00	0.0%	1.01	153.95	0.0%	1.01	134.76	0.0%	1.01	202.64	−0.2%	1.01	162.54	0.1%
0.0%	1.05	8.23	0.0%	1.05	8.23	0.0%	1.05	28.33	0.0%				1.05	28.33	0.0%			
0.0%	1.03	3.13	0.0%	1.03	1.98	0.0%	1.03	22.72	0.0%				1.03	49.46	0.0%			
0.0%	1.04	1.70	0.0%	1.04	2.00	0.0%	1.04	16.01	0.0%				1.04	35.06	0.2%			
0.0%	1.03	1.20	0.0%	1.03	1.60	0.0%	1.03	4.30	0.0%				1.03	17.00	0.0%			
0.0%	1.05	2.00	0.0%	1.05	3.50	0.0%				1.05	5.99	−0.1%				1.05	11.00	0.0%
0.1%	1.05	3.00	0.0%	1.05	4.00	0.0%				1.05	30.02	0.1%				1.05	80.00	0.0%
	1.10	22.15		1.10	57.49		1.10	87.54		1.10	97.12		1.10	55.54		1.10	41.39	
	1.10	33.67		1.10	73.10		1.10	79.49		1.10	65.03		1.10	80.91		1.10	68.41	
0.3%	1.42	1825.00	0.6%	1.39	3680.99	0.8%	1.37	6824.65	0.9%	1.37	6230.34	0.1%	1.39	9368.00	0.2%	1.39	6864.09	0.1%
0.3%	1.03	5.00	0.0%	1.03	7.00	0.0%	1.03	10.00	0.0%	1.02	9.01	0.1%	1.03	13.99	0.0%	1.02	13.02	0.1%
0.0%	1.04	1245.00	0.0%	1.04	1309.90	0.0%	1.04	1420.40	0.0%	1.04	1298.22	−0.1%	1.04	1450.68	0.0%	1.04	1302.78	0.2%
	0.96	0.95		0.96	7.65		0.94	15.02	0.1%	0.94	249.79	−0.1%	0.94	25.00	0.0%	0.94	500.21	0.0%
	1.10	6.81		1.10	5.58		1.10	9.20		1.10	9.20		1.10	25.87		1.10	9.47	
	1.05	5.39		1.05	7.32		1.05	6.07		1.05	4.63		1.05	15.31		1.05	13.54	

	UFH05MF			*UFH10MF*			*UFH15M*			*UFH15F*			*UFHADM*			*UFHADF*		
%Diff	**Density**	**Mass**	**%Diff**	**Density**	**Mass**	**%Diff**	**Density**	**Mass**	**%Diff**	**Density**	**Mass**	**%Diff**	**Density**	**Mass**	**%Diff**	**Density**	**Mass**	**%Diff**
0.0%	1.03	11.00	0.0%	1.03	12.00	0.0%	1.03	13.01	0.1%	1.02	13.01	0.0%	1.03	15.00	0.0%	1.02	14.98	−0.1%
0.0%	1.07	0.33	0.9%	1.07	0.36	0.0%	1.07	0.49	0.0%	1.07	0.39	−0.3%	1.07	0.45	0.1%	1.07	0.45	−0.1%
0.0%	1.03	0.25	0.0%	1.03	0.35	0.0%	1.03	0.50	0.5%	1.02	0.50	0.2%	1.03	0.60	0.2%	1.02	0.60	0.2%
	1.04	33.23		1.04	72.49		1.04	70.31		1.04	67.75		1.04	0.00		1.04	48.83	
0.0%	1.06	50.00	0.0%	1.06	80.01	0.0%	1.06	130.00	0.0%	1.06	130.04	0.0%	1.06	150.05	0.0%	1.06	130.15	0.1%
	1.65	15.00	0.0%	2.33	29.99	0.0%	3.00	44.99	0.0%	3.00	35.22	0.6%	3.00	50.01	0.0%	3.00	39.99	0.0%
−46.4%	1.03	30.00	0.0%	1.03	37.50	0.0%	1.03	34.99	0.0%	1.03	30.02	0.1%	1.03	24.97	−0.1%	1.03	20.01	0.0%
0.0%	1.05	3.40	0.0%	1.05	7.90	0.0%	1.05	12.02	0.2%	1.05	12.02	0.2%	1.05	20.05	0.2%	1.05	17.00	0.0%

ted as per section 5.3.3 of ICRP 89

d was matched to within 1% of the reference volume calculated as per section 6.3.2 of ICRP 89.

nly when the calculated density (= reference mass / model volume) was less than unity.

region was matched to reference masses calculated as per section 8.2.1 of ICRP89

ne cranium is not fully ossified at these ages.

Residual Soft Tissue in other older phantoms.

trabecular bone), bone marrow (active and inactive), and miscellaneous skeletal tissues as per section 9.2.15

Phys Med Biol. Author manuscript; available in PMC 2010 January 21.

6

ence values for tissues in the UF hybrid-voxel phantom series.

UFH05MF			*UFH10MF*			*UFH15M*			*UFH15F*			*UFHADM*			*UFHADF*		
Density	**Mass**	**%Diff**	**Density**	**Mass**	**%Diff**	**Density**	**Mass**	**%Diff**	**Density**	**Mass**	**%Diff**	**Density**	**Mass**	**%Diff**	**Density**	**Mass**	**%Diff**
1.03	0.45	0.0%	1.03	0.46	0.0%	1.03	2.06	0.0%	1.02	0.46	0.0%	1.03	2.02	0.0%	1.02	0.64	0.0%
1.03	8.73	0.0%	1.03	8.55	0.0%	1.03	9.65	0.0%	1.02	8.43	0.0%	1.03	16.57	0.0%	1.02	9.07	0.0%
1.03	1.77	0.0%	1.03	1.10	0.0%	1.03	5.04	0.0%	1.02	7.75	0.0%	1.03	2.24	0.0%	1.02	1.92	0.0%
1.07	6.24	−0.9%	1.07	11.97	−0.3%	1.07	21.85	−0.7%	1.07	14.88	−0.8%	1.07	28.23	0.8%	1.07	19.03	0.2%
1.03	2.20	0.0%	1.03	2.02	0.0%	1.03	2.86	0.0%	1.02	2.73	0.0%	1.03	2.28	0.0%	1.02	1.47	0.0%
1.07	4.19	−0.3%	1.07	4.48	−0.3%	1.07	7.49	−0.1%	1.07	5.96	−0.7%	1.07	9.96	−0.4%	1.07	8.01	0.1%
1.07	3.00	0.0%	1.07	3.54	0.0%	1.07	8.01	0.0%	1.07	7.37	0.0%	1.07	15.49	0.0%	1.07	9.63	0.0%
0.39	298.63	−0.5%	0.33	498.15	−0.4%	0.32	898.66	−0.1%	0.31	747.03	−0.4%	0.33	1196.37	−0.3%	0.34	947.88	−0.2%
1.05	12.97	−0.1%	1.05	31.93	−0.2%	1.05	55.84	−0.3%	1.05	52.87	−0.3%	1.05	72.56	−0.6%	1.05	59.87	−0.2%
1.03	33.97	−0.1%	1.03	43.94	−0.1%	1.03	68.00	0.0%	1.02	64.77	−0.4%	1.03	84.89	−0.1%	1.02	69.80	−0.3%
1.03	1.99	−0.6%	1.03	2.98	−0.7%	1.03	2.98	−0.6%	1.02	3.00	0.0%	1.03	2.98	−0.8%	1.02	3.00	−0.2%
1.03	9.99	−0.1%	1.03	17.97	−0.2%	1.03	29.85	−0.5%	1.03	29.98	−0.1%	1.03	40.03	0.1%	1.03	34.88	−0.4%
1.03	45.55	−0.3%	1.03	84.77	−0.3%	1.03	119.46	−0.5%	1.03	119.72	−0.2%	1.03	150.11	0.1%	1.03	139.61	−0.3%
1.03	81.03	−0.6%	1.03	116.02	−0.8%	1.03	199.66	−0.2%	1.02	199.51	−0.2%	1.03	249.71	−0.1%	1.02	230.21	0.1%
1.03	213.66	−2.9%	1.03	359.92	−2.7%	1.03	506.82	−2.5%	1.03	503.38	−3.2%	1.03	633.67	−2.5%	1.03	581.96	−3.0%
1.03	32.78	−66.9%	0.54	162.62	−0.2%	0.41	267.80	−4.4%	0.45	278.99	−0.4%	0.44	349.00	−0.3%	0.52	279.88	0.0%
1.03	48.75	−0.5%	1.03	84.83	−0.2%	1.03	121.53	−0.4%	1.03	121.66	−0.3%	1.03	149.27	−0.5%	1.03	144.39	−0.4%
1.03	27.09	−45.8%	1.03	28.16	−59.8%	1.03	72.36	−39.7%	1.02	43.81	−63.5%	1.03	100.50	−33.0%	1.02	51.61	−67.7%
1.03	48.86	−0.3%	1.03	84.63	−0.4%	1.03	121.64	−0.3%	1.03	121.66	−0.3%	1.03	149.57	−0.3%	1.03	144.69	−0.2%
0.76	24.92	−0.3%	0.49	16.52	−52.8%	0.34	30.32	−49.5%	0.98	59.73	−0.4%	1.03	55.19	−26.4%	1.08	79.78	−0.3%
1.03	21.85	−0.7%	1.03	39.89	−0.3%	1.03	55.54	−0.8%	1.03	55.81	−0.3%	1.03	69.77	−0.3%	1.03	69.93	−0.1%
0.86	24.92	−0.3%	1.03	31.90	−8.9%	0.49	39.42	−34.3%	1.02	52.01	−13.3%	0.97	74.86	−0.2%	1.02	56.27	−29.7%
1.05	564.82	−0.9%	1.05	828.83	−0.1%	1.05	1298.08	−0.1%	1.05	1299.07	−0.1%	1.06	1798.48	−0.1%	1.06	1396.14	−0.3%
1.03	2.58	−0.8%	1.03	4.41	0.3%	1.03	7.65	−0.7%	1.02	7.28	−0.3%	1.03	9.93	−0.7%	1.02	7.95	−0.6%

UFH05MF			*UFH10MF*			*UFH15M*			*UFH15F*			*UFHADM*			*UFHADF*		
Density	**Mass**	**%Diff**	**Density**	**Mass**	**%Diff**	**Density**	**Mass**	**%Diff**	**Density**	**Mass**	**%Diff**	**Density**	**Mass**	**%Diff**	**Density**	**Mass**	**%Diff**
1.03	14.96	−0.3%	1.03	25.95	−0.2%	1.03	44.96	−0.1%	1.02	41.89	−0.3%	1.03	58.14	0.2%	1.02	47.91	−0.2%
1.03	34.95	−0.2%	1.03	59.93	−0.1%	1.03	109.60	−0.4%	1.02	99.91	−0.1%	1.03	139.26	−0.5%	1.02	119.89	−0.1%
1.04	84.61	−0.5%	1.04	139.37	−0.4%	1.04	228.88	−0.5%	1.04	219.73	−0.1%	1.05	330.45	0.1%	1.05	249.50	−0.2%
1.06	134.76	−0.2%	1.06	229.79	−0.1%	1.06	428.82	−0.3%	1.06	319.56	−0.1%	1.06	508.31	−0.3%	1.06	369.16	−0.2%
1.04	102.44	−0.5%	1.04	179.81	−0.1%	1.04	249.39	−0.2%	1.04	239.31	−0.3%	1.05	308.91	−0.4%	1.05	274.38	−0.2%
1.01	5.62	−0.1%	1.01	9.19	−0.1%	1.01	12.77	0.0%	1.01	12.24	−0.2%	1.01	15.60	−0.6%	1.01	13.91	−0.1%
1.04	15.92	−0.5%	1.04	24.85	−0.6%	1.04	39.85	−0.4%	1.04	34.83	−0.5%	1.04	49.76	−0.5%	1.04	40.00	0.0%
1.01	61.67	−0.5%	1.01	98.59	−0.4%	1.01	153.39	−0.4%	1.01	134.24	−0.4%	1.01	201.77	−0.6%	1.01	161.76	−0.4%
1.05	3.56	0.0%	1.05	6.05	0.0%	1.05	28.68	0.0%				1.05	20.33	0.0%			
1.03	1.15	0.0%	1.03	1.71	0.0%	1.03	17.78	0.0%				1.03	34.99	0.0%			
1.04	1.68	−0.9%	1.04	2.00	−0.2%	1.04	15.90	−0.6%				1.04	34.93	−0.2%			
1.03	1.20	0.0%	1.03	1.59	−0.5%	1.03	4.29	−0.2%				1.03	16.96	−0.2%			
1.05	1.90	0.2%	1.05	3.48	−0.6%				1.05	5.96	−0.6%				1.05	10.97	−0.3%
1.05	1.30	−0.2%	1.05	3.98	−0.5%				1.05	29.95	−0.2%				1.05	79.95	−0.1%
1.10	2.96		1.10	57.59		1.10	81.65		1.10	86.82		1.10	51.52		1.10	38.00	
1.10	3.91		1.10	72.06		1.10	62.90		1.10	59.27		1.10	70.49		1.10	54.05	
1.42	1805.24	−0.5%	1.39	3650.02	0.0%	1.37	6752.21	−0.2%	1.37	6180.40	−0.7%	1.39	9317.24	−0.4%	1.39	6814.37	−0.7%
1.10	610.13	7.0%	1.10	1137.44	38.7%	1.10	2295.58	14.8%	1.10	1927.02	13.4%	1.10	3687.36	11.7%	1.10	2553.04	11.0%
1.03	5.01	0.1%	1.03	6.98	−0.3%	1.03	10.01	0.1%	1.02	9.01	0.1%	1.03	13.89	−0.8%	1.02	12.99	−0.1%
1.04	1244.72	0.0%	1.04	1309.47	0.0%	1.04	1418.71	−0.1%	1.04	1295.73	−0.3%	1.04	1449.55	0.0%	1.04	1287.72	−0.9%
0.96	0.94		0.96	7.63		0.94	14.96	−0.3%	0.94	249.02	−0.4%	0.94	24.88	−0.5%	0.94	498.70	−0.3%
1.10	5.13		1.10	3.17		1.10	5.90		1.10	6.91		1.10	9.09		1.10	5.68	
1.05	3.57		1.05	6.52		1.05	3.65		1.05	3.35		1.05	7.61		1.05	13.84	

Phys Med Biol. Author manuscript; available in PMC 2010 January 21.

UFH05MF			*UFH10MF*			*UFH15M*			*UFH15F*			*UFHADM*			*UFHADF*		
Density	**Mass**	**%Diff**	**Density**	**Mass**	**%Diff**	**Density**	**Mass**	**%Diff**	**Density**	**Mass**	**%Diff**	**Density**	**Mass**	**%Diff**	**Density**	**Mass**	**%Diff**
1.03	10.95	−0.5%	1.03	11.96	−0.4%	1.03	12.95	−0.4%	1.02	12.93	−0.5%	1.03	14.87	−0.8%	1.02	14.89	−0.7%
1.07	0.33	−0.1%	1.07	0.36	0.4%	1.07	0.51	0.0%	1.07	0.39	0.1%	1.07	0.45	−0.8%	1.07	0.45	0.8%
1.03	0.25	0.2%	1.03	0.35	−0.7%	1.03	0.49	−1.1%	1.02	0.50	−0.5%	1.03	0.60	0.0%	1.02	0.60	0.7%
1.04	31.57		1.04	68.89		1.04	47.87		1.04	56.63		1.04	73.18		1.04	46.99	
1.06	49.90	−0.2%	1.06	79.80	−0.2%	1.06	129.04	−0.7%	1.06	129.06	−0.7%	1.06	149.90	−0.1%	1.06	129.80	−0.2%
1.65	14.92	−0.6%	2.33	29.98	−0.1%	3.00	44.90	−0.2%	3.00	35.23	0.6%	3.00	49.56	−0.9%	3.00	40.64	1.6%
1.03	23.35	−0.2%	1.03	37.46	−0.1%	1.03	34.98	−0.1%	1.03	29.96	−0.1%	1.03	24.92	−0.3%	1.03	19.91	−0.5%
1.05	7.40	−0.1%	1.05	7.90	0.0%	1.05	12.00	0.0%	1.05	11.83	−1.4%	1.05	19.97	−0.1%	1.05	16.91	−0.6%
1.01	12266.07	−1.3%	1.02	22692.42	0.0%	1.03	40681.58	1.5%	1.01	38367.10	0.4%	1.02	51489.60	0.9%	1.00	42484.88	−0.5%
	17.84	−0.6%		31.85	1.3%		55.99	1.7%					72.28	1.2%			
	18.12	−1.1%		32.34	1.0%		56.81	1.4%					73.39	1.0%			
	17.85	−0.5%		31.86	1.3%					52.50	0.8%					58.80	0.1%
	18.13	−1.1%		32.35	1.1%					53.33	0.6%					59.73	−0.2%

tissues, fixed lymphatic tissues, blood vessels, and miscellaneous tissues. Miscellaneous tissues